Numerical Modelling for Process Investigation of a Single Coal Particle Combustion and Gasification

Tata Sutardi, Manosh C. Paul, Nader Karimi, and Paul L. Younger

Abstract - Combustion and Gasification are commercial processes of coal utilization, and therefore continuous improvement is needed for these applications. The difference between these processes is the reaction mechanism, in the case of combustion the reaction products are CO_2 and H_2O, whereas in the case of gasification the products are CO, H_2 and CH_4. In order to investigate these processes further, a single coal particle model has been developed. The definition of the chemical reactions for each process is key for model development. The developed numerical model simulation uses CFD (Computational Fluid Dynamic) techniques with an Eddy Break Up (EBU) model and a kinetics parameter for controlling the process reaction. The combustion model has been validated and extended to model the gasification process by inclusion of an additional chemical reaction. Finally, it is shown that the single coal particle model could describe single coal particle combustion and gasification. From the result, the difference between single coal particle combustion and gasification can clearly be seen. This simulation model can be considered for further investigation of coal combustion and gasification application processes.

Keywords: Combustion, gasification, numerical model, kinetics model.

I. INTRODUCTION

Coal continues to be the largest fuel used for electricity generation worldwide based on the IEO (International Energy Outlook) 2016, which accounted for 40% of total world electricity generation in 2012, will decline to 29% of the total in 2040, despite a continued increase in total coal-fired electricity generation from 8.6 trillion kWh in 2012 to 9.7 trillion kWh in 2020 and 10.6 trillion kWh in 2040 [1]. Total electricity generation from coal in 2040 is predicted 23% above the 2012 in total. Otherwise, coal also has been developed through gasification process either for electricity generation or chemical stocks and other utilization, which is expected the future potency of coal utilization could be more promising.

Since combustion and gasification are dominating in the coal utilization, the development of research and application for these processes are keep growing. In combustion, the developments are mostly on the optimization process, while in the gasification they at on the better mechanisms to achieve the end products. To support this, the single coal particle simulation model has been developed in this research. This modelling process is commonly used for simulating either combustion or gasification, and the result could be considered as initial identification before they are used in further application. In this research, the combustion simulation result has been validated with the experimental data, and the gasification has been modelled by defining more chemical reactions. The objective of this paper is giving the description of coal combustion and gasification through a single coal particle model investigation. This understanding is important to be used for further development.

II. SIMULATION MODEL DEVELOPMENT

The single coal particle combustion and gasification processes occur in the drop tube furnace (DTF). Computational physical geometry of the furnace is illustrated in Fig. 1 [2].

The DTF is represented by a cylindrical shape geometry as illustrated in Fig. 1(a), with the inlet diameter of 7 cm, and the hot wall furnace length of 25 cm from the inlet. The coal particle injection starts from the centre of the inlet. The axi-symmetric model with grid distribution used for the simulation can be seen in Fig. 1(b).
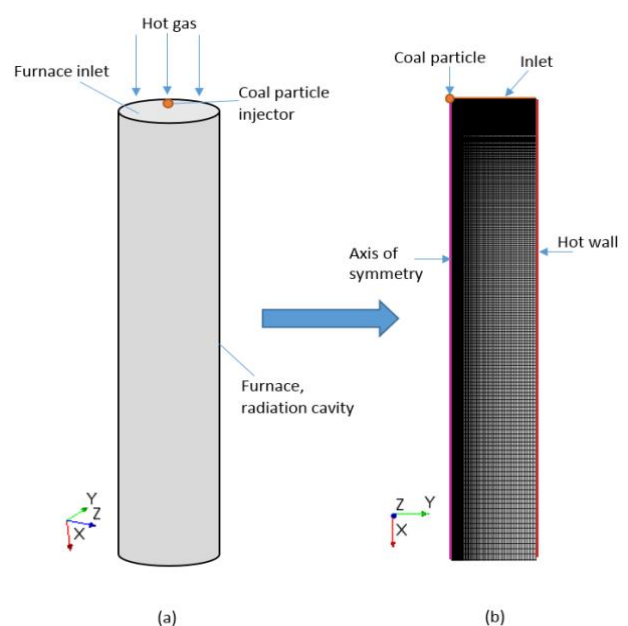

Fig. 1. An illustration of the geometry model, (a) cylindrical shape and (b) axi-symmetric model with grid

TABLE I.
COAL COMBUSTION AND GASIFICATION REACTIONS

Mechanism	Reaction no	Kinetic parameter			Ref
		A (vary)	E_a (j/kmol)	β	
Rawcoal $\rightarrow$ YY Coal volatile + (1 –YY)	R1	3.12 E+05	7.4 E+07	0	[3]
$C + O_2 \rightarrow CO_2$	R2	2 E+1	7.9 E+07	0	[4]
$C + 0.5O_2 \rightarrow CO$	R3	1 E+3	1.33 E+08	1	[4]
$C + CO_2 \rightarrow 2CO$	R4	4.4	1.62 E+08	1	[5]
$C + H_2O \rightarrow CO + H_2$	R5	1.33	1.47 E+08	1	[5]
$C + 2H_2 \rightarrow CH_4$	R6	1 E+3	1.131 E+08	0	[6]
Coal Volatile + $O_2 \rightarrow CO_2 + H_2O + N_2$	R7	2.119	2.027 E+08	0	[3]
$CO + 0.5O_2 \rightarrow CO_2$	R8	1.3 E+11	1.26 E+08	0	[7]
$H_2 + 0.5O_2 \rightarrow H_2O$	R9	1.5 E+13	2.85 E+08	0	[6]
$CO + H_2O \rightarrow CO2 + H_2$	R10	4.2 E+07	1.383 E+08	0	[6]
$CH_4 + H_2O \rightarrow CO + 3H_2$	R11	4.4 E+11	1.68 E+08	0	[6]
$CH_4 + 0.5O_2 \rightarrow CO + 2H_2$	R12	3 E+08	1.26 E+08	-1	[6]
$CH_4 + CO_2 \rightarrow 2CO + 2H_2$	R13	4.6 E+11	3.124 E+08	0.3	[8]

In the simulation, seven reactions are used for representing the coal combustion process and thirteen reactions for representing the gasification reaction mechanism. Those reactions are presented in TABLE I.[9]. The combustion reactions consist of R1, R2, R3, R4, R5, R7, and R8, and the gasification reactions are defined in TABLE I. Eddy Break Up (EBU) with a kinetic parameter model is used for controlling the chemical reaction mechanism. For the particle transport and transformation, a Lagrangian approach with multi-phase method is used, as the coal particle consists of several components.

The mechanisms of the coal particle conversion are described through the several equations as follows.

The continuity of mass of the coal particle p is described as

$$\frac{dm_p}{dt} = -r_p \qquad (1)$$

where, the net rate for raw coal consumption is given by

$$r_p = k_1 \alpha_p m_p \qquad (2)$$

And the rate of production for coal volatile is described as

$$r_{vm} = k_1 YY \alpha_p m_p \qquad (3)$$

Then, the reaction rate coefficient is the Arrhenius form given by

$$k_1 = AT^\beta exp\left(\frac{-E_a}{RT}\right) \qquad (4)$$

Particle and gas reactions begin after the volatile fraction of raw coal particle completely evolved. This heterogeneous reaction rate is determined by combining the effect of the Arrhenius rate and diffusion coefficient, and for this case the constant diffusion coefficient is assigned as 4.5E-5 m^2/s. The model of particle rate consumption is then determined by

$$r = \frac{dm_i}{dt} = -\frac{k_m k}{k + k_m} \emptyset C_g M_w A_p \qquad (5)$$

where,

$$k_m = \frac{(Sh)(D_m)}{d} \qquad (6)$$

The reaction rate of each gas and gas (homogeneous) reactions (R7 to R13) is a function of the composition and rate constant, given by the expression:

$$R_j = R_{i,kin} = -k_j \prod_{all\ reactants} \left(\frac{\rho Y_i}{M_i}\right)^{p_{ij}} \qquad (7)$$

The equation of motion for the particle is defined as,

$$m_p \frac{d\overline{u_{i,J,k}^p}}{dt} = \sum \bar{F} \qquad (8)$$

Since the particle size in this simulation is small, so the lift force of the particle is neglected. In the meanwhile, the effect of drag and gravity force has been used in this simulation since these forces could have influenced the parameter of investigation.

A. *Governing equation*

In homogenous reacting flow, the change of pressure, temperature, velocity, and concentration of species are the results of fluid flow, molecular transport, radiation and chemical reaction. In order to consider these effect on the simulation model, a set of mathematical modelling defined, which consist of Navier–Stokes equation (conservation of mass, momentum, and stress tensor), species mass conservation, and energy conservation equation. These equations are developed by considering a control volume as a system.

The law of mass conservation results in the mass continuity equation as shown below:

$$\frac{\partial \rho}{\partial t} + \frac{\partial (\rho u_i)}{\partial x_i} = 0 \qquad (9)$$

The equation for the conservation of momentum is represented by [10]:

$$\frac{\partial (\rho u_i)}{\partial t} + \frac{\partial (\rho u_i u_j)}{\partial x_j} = \frac{\partial p}{\partial x_i} + \frac{\partial \tau_{ij}}{\partial x_j} + \rho g_i \qquad (10)$$

where p is the static pressure, τ_{ij} is the stress tensor, ρg_i is the gravitational body force. The stress tensor τ_{ij} for a Newtonian fluid is defined by [10]:

$$\tau_{ij} = \left[\mu\left(\frac{\partial u_i}{\partial x_j} + \frac{\partial u_j}{\partial x_i}\right)\right] - \frac{2}{3}\mu \frac{\partial u_l}{\partial x_l}\delta_{ij} \qquad (11)$$

The concentration of each species can be expressed in terms of the mass fraction $m_i(x,t)$, or the concentration of

species $C_i = m_i \rho$, which is defined as the mass of species per unit volume.

The conservation law of chemical species is represented as,

$$\frac{\partial}{\partial t}(\rho m_i) + \nabla \cdot (\rho m_i V + J_i) = R_i \qquad (12)$$

Where R_i is the account for the production or consumption of the species by chemical reactions.

The energy equation in this simulation may be written as [10]:

$$\frac{\partial(\rho h)}{\partial t} + \frac{\partial(\rho u_i h)}{\partial x_i} = \frac{\partial}{\partial x_i} \lambda \frac{\partial T}{\partial x_i} - \frac{\partial \sum_j h_j J_j}{\partial x_i} + \frac{Dp}{Dt} + (\tau_{ik})\frac{\partial u_i}{\partial x_k} + h_s \qquad (13)$$

In this equation h is the enthalpy and h_s includes heat of chemical reaction, any inter-phase exchange of heat, and any other user defined volumetric heat sources.

In this simulation, the equation state of gas in the reaction is treated as ideal gas. This equation is needed to connect the thermodynamic variables such as, $p, \rho,$ and T. The ideal gas equation is expressed as

$$\frac{p}{\rho} = RT \qquad (14)$$

R is universal gas constant.

In turbulent flows, all transport processes are enhanced by turbulent fluctuations. When the interaction of a flame and a turbulent flow occurs, the turbulence is modified by the combustion due to the strong flow accelerations through the flame front induced by the release of heat and due to the large kinematic viscosity changes associated with the temperature changes. Turbulence causes large fluctuations of mass fractions, temperature and density and moreover extinction can occur when turbulence effects are strong. Turbulent flows are characterized by the presence of a wide range of time and scales at which motion and fluctuations take place.

In this simulation, the RANS (Reynolds-Averaged Navier-Stokes) approach is used for solving the turbulence effect on the species transport. These equations describe the behaviour of the time-averaged flow quantities instead of the exact instantaneous values. In this approach, RANS equations arise when the Reynolds decomposition is implemented into the Navier-Stokes equations.

The RANS equation is represented as,

$$\frac{\partial(u_i)}{\partial t} + \rho \frac{\partial((u_i u_j))}{\partial x_j}$$
$$= -\frac{\partial(p)}{\partial x_i}$$
$$+ \frac{\partial}{\partial x_j}\left[\mu\left(\frac{\partial}{\partial x_j}u_i + \frac{\partial}{\partial x_i}u_j\right.\right.$$
$$\left.\left. - \frac{2\partial}{3\partial x_k}u_k \delta_{i,j}\right)\right] - \frac{\partial \tau_{ij}}{\partial x_j} \qquad (15)$$

The equations above are not closed because the component Reynold stress tensor τ_{ij}, is unknown and cannot be expressed as function of (u) and (p). In order to solve this equation, so the transport equation model is needed, and this simulation uses the realizable $k - \varepsilon$ model. The k model is transport equation for turbulent kinetic energy, and may be represented as

$$\rho \frac{\partial k}{\partial t} + \rho(u_j)\frac{\partial k}{\partial x_j} = 2\mu(S_{ij})\frac{\partial(u_i)}{\partial x_j} - \rho\varepsilon$$
$$+ \frac{\partial}{\partial x_j}\left[\left(\mu + \frac{\mu_t}{\sigma_k}\right)\frac{\partial k}{\partial x_j}\right] \qquad (16)$$

while, the ε model is transport equation for viscous dissipation (the rate at which the kinetic energy of small scale fluctuation is converted into heat by viscous friction, and it represented as,

$$\rho\frac{\partial\varepsilon}{\partial t} + \rho(u_j)\frac{\partial\varepsilon}{\partial x_j} = C_{\varepsilon 1}P_k\frac{\varepsilon}{k} - C_{\varepsilon 2}\rho\frac{\varepsilon^2}{k}$$
$$+ \frac{\partial}{\partial x_j}\left[\left(\mu + \frac{\mu_t}{\sigma_\varepsilon}\right)\frac{\partial\varepsilon}{\partial x_j}\right] \qquad (17)$$

In this simulation the constant used for the equation above are: $C_{\varepsilon 1} = 1.44$; $C_{\varepsilon 2} = 1.9$; $\sigma_k = 1$; $\sigma_\varepsilon = 1.2$

B. Simulation Procedures and Boundary conditions

The initial boundary conditions are taken from an experimental study [2]. The furnace was heated up with hot air before the injection of the coal particle. The inlet condition was set as a velocity inlet, with an initial temperature of hot air of 1200K, and at the same time the furnace wall temperature was at 1400K. The inlet air with a velocity of 0.045 m/s was injected through the furnace's inlet until the flow becomes fully developed and steady-state. Moreover, in order to accommodate the fully development region, the furnace wall was extended to 75 cm and it set as an isolator.

In the simulations, a type of coal namely PSOC 1451 is used, and identified as bituminous coal. The chemical properties of these coals are taken from the proximate and ultimate analyses and presented in TABLE II. [2].

TABLE II.
COAL CHEMICAL COMPOSITIONS

	PSOC 1451
Proximate Analysis as receives	
Moisture (%)	2.5
Volatile matter (%)	33.6
Fixed Carbon (%)	50.6
Ash (%)	13.3
Ultimate Analysis (dry basis)	
Carbon (%)	71.9
Hydrogen (%)	4.9
Oxygen (%) (by diff.)	6.9
Nitrogen (%)	1.4
Sulfur (%)	1.4
Sodium (%)	0.06
Ash (%)	13.7
Heating value dry fuel (MJ/kg)	31.5

In this simulation it is needed to define raw coal particle and coal volatile composition, and based on the proximate and ultimate correlations, the coal volatile composition for PSOC 1451 is defined as $CH_{2.7}O_{0.248}N_{0.058}$ or the *YY* value of 0.29 as stated in the reaction balance equation R1[11].

III. VALIDATION AND COMPARISON RESULT

The simulation is developed based on the experimental procedures of as mentioned in previous section. In this section, the simulation results of coal particle combustion are compared with the experimental result for validation purposes. The validation process is necessary to be described for giving understanding on mechanism behaviour of both processes. The valid model is then applied on the coal particle gasification process.

A. Single coal particle combustion model validation

This single coal particle combustion simulation model has been validated by comparing the results with the existing experimental data from an experiment of coal combustion [2]. The temperature profile of the coal particle after ignition from the simulation and experimental are shown in Fig. 2.
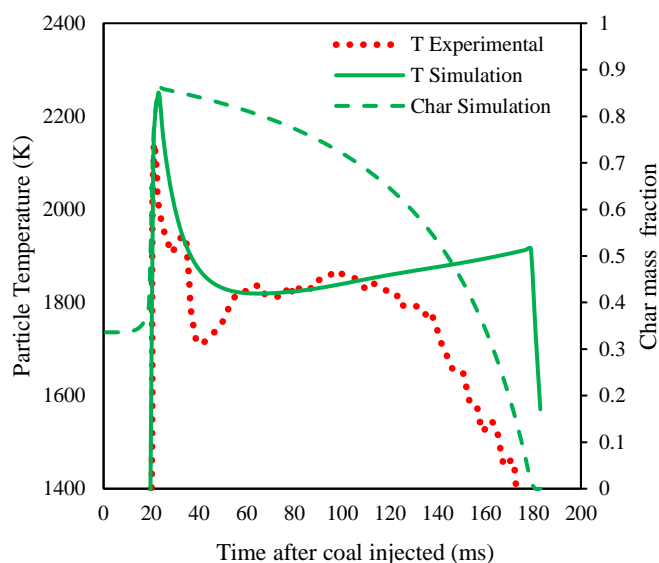

Fig. 2. Validation result of coal particle combustion

The numerical temperature profile of the coal particle is in good agreement with the experimental data. The trend is captured reasonably well and the burn-out time (better seen by the profile of char mass fraction) is almost exactly the same as in the experimental. Further, the maximum temperature attained by the simulated coal volatile combustion (~2250K) and simulated char combustion (~1910K) are also in good agreement with the experimental values, which are (~2200K) and (~1870K), respectively. These differences can be tolerated since the particle burn-out time obtained from the simulation of 160ms agrees very well with the actual burn-out time from the experiment. Thus, overall, the combustion model is capturing the real behaviour well.

Now that the combustion process has been validated, the model is extended to simulate the gasification process. The key difference of this process is in the reaction mechanism as mentioned in the previous section. As an aim of this paper for obtaining the comparison process between the combustion and gasification mechanisms, so the comparison result of a single coal particle combustion and gasification are described on the next section.

B. Comparison Result

The results of both processes are compared in order to describe and identify each process mechanism. The parameters that will be compared are the particle temperature

and coal volatile fraction, the gas products CO and CO_2, and gas products H_2 and H_2O.

Particle temperature and coal volatile comparison

By using the same type of coal for each process, the particle temperature and coal volatile fraction of a single coal particle combustion and gasification comparison can be seen in the Fig. 3.
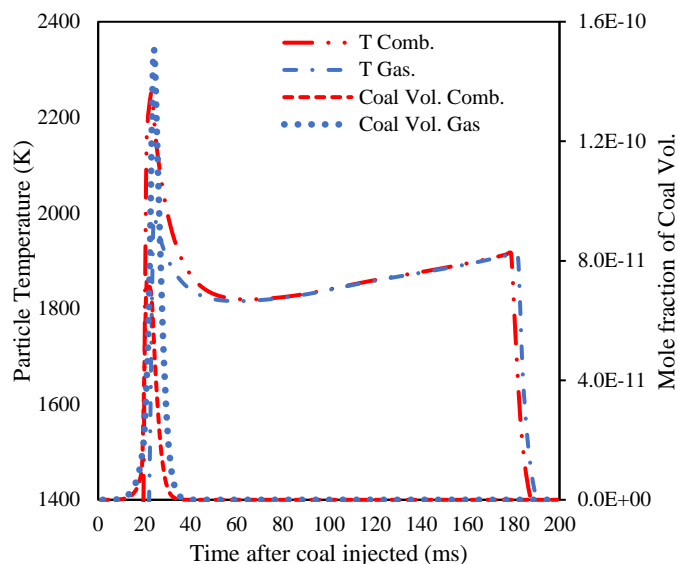

Fig. 3. The temperature and coal volatile mole fraction comparison

From Fig. 3, it can be seen that during the devolatilization process which occurs between times 20 and 40ms after the coal is injected, the coal particle combustion temperature is higher than in the case of gasification, but after this process particle temperature is relatively the same for both cases. Furthermore the burn out time of the gasification process is slightly longer than that of the combustion process.

The coal volatile reaction in the case of the combustion process is slightly faster than in the case of the gasification process. This is because, the coal volatile during the gasification process is reacting not only with oxygen (oxidation) but also with other gas species (pyrolysis). After coal volatile reaction process completed, the both reactions of coal volatile stop since there is no more coal volatile there.

CO and CO_2 comparison

As defined in both reactions of TABLE I, the single coal particle combustion and gasification produce CO and CO_2. The comparison of these gaseous productions of each process can be seen in the Fig. 4.

From Fig. 4, it can be seen that, overall, the CO production during the gasification process is higher than in the combustion case. The overhead occurs because of the char reaction. As defined in the reaction, CO potentially produced when the char reacted with O_2, CO_2, or H_2O. After the char burn out, the CO production stop. At ~180ms, the CO_2 production of the two processes stabilizes but since more CO is converted into CO_2 in the gasification, the CO_2 is higher than in the combustion.

For the CO_2 formation, it can be seen the gap of each process occurs after devolatilization stage, and as identified above, the CO_2 production comes from the CO and O_2 reaction. In this single coal particle model, the supply of O_2 is not limited in order to see the reactivity of reaction mechanism.
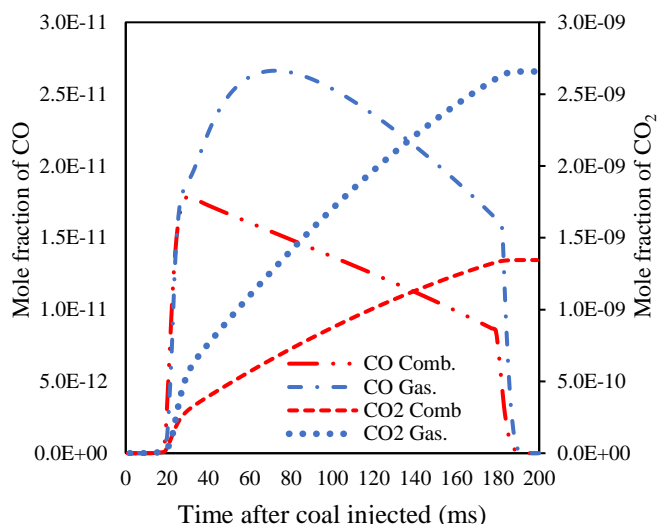
Fig. 4. The comparison for CO and CO_2

The understanding of the CO and CO_2 formation in this section is important and can be considered for further gasification process. In the gasification process, the more O_2 at some point of reaction could cause more CO_2 production rather than CO which is more preferable.

H_2 and H_2O comparison

H_2 and H_2O formation are defined in the reaction mechanism as in TABLE I. In order to investigate the formation mechanism through the single coal particle model, so the comparison of these gas production will be compared in this section. The comparison of H_2 and H_2O formation on a single coal particle combustion and gasification, can be seen in the Fig. 5.
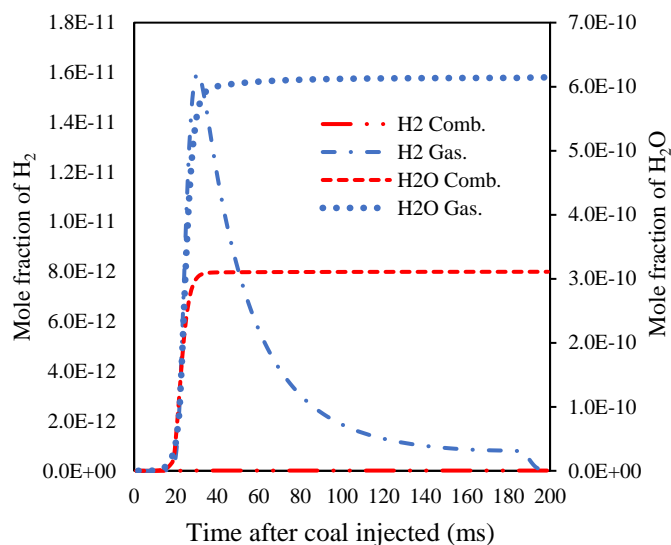

Fig. 5. The comparison for H_2 and H_2O

From Fig. 5, it can be seen that the H_2 production of the gasification process is higher than the combustion, and it is produced in the devolatilization stage. It is known that in the coal volatile oxidation, the H_2O is produced as seen in the R7 and it seems to occur simultaneously with the H_2. Comparing Fig. 5 and Fig. 3 it can be seen that the increasing trend of coal volatile and H_2 are similar, but in the decreasing trend are slightly different. The decreasing of H_2 is slower than coal

volatile. For the combustion process, the H_2 production from the single coal particle combustion model is very low and almost couldn't be identified in Fig. 5.

For the H_2O production, it can be seen the overhead of H_2O production occurs in the time 20 to 40ms, during which the devolatilization reaction occurs. After this stage, the H_2O in both processes stabilizes. From this phenomenon it can be considered that the H_2O formation in the gasification process occurs because of oxidation of H_2 in the devolatilization stage. During the char reaction, the mole fraction of H_2O is stable but H_2 is decreasing since it reacted more with char to produce CH_4; this is because, the H_2 is decreasing without affecting the production of H_2O. In the comparison, this paper does not consider the CH_4 formation is not considered since it's reaction is not defined in the combustion process.

From the H_2 and H_2O formation as described in this section, it is important to be consider to add more H_2O for increasing H_2 production in coal gasification process, and also to keep char appear in the reaction in order to for the products such as H_2 and CH_4.

IV. CONCLUSION

The single coal particle model of combustion and gasification has been developed and considered for developing better process of coal combustion and gasification. For combustion application, this model could be used for estimating burn out time of pulveriser coal combustion, which affects the design and optimization of a burner. For the gasification, this model can be used as a consideration for developing better gas products formation by identifying the control parameter that affects the process.

From the simulation of a single coal particle combustion and gasification, it can be seen the process comparison of the reaction mechanism and how it affects the gas products formation for each process. It also could be understood if the H_2 products come from the H_2O that is produced in the reaction and this information could be the main reason of increasing H_2O fraction for producing more H_2.

The correlation of char appearance in the coal particle combustion and gasification also can be observed through this simulation result. In the gasification, the appearance of char give beneficiary for producing the CO as an expected products. The simulation result shows after this char burn-out, and at the condition of O_2 exceeding the stoichiometric reaction demand, it potentially reacts with CO into CO_2.

Since this model used a single coal particle which it's mole fraction far below the O_2 mole fraction, so the excess of O_2 occur in the reaction. Because of it, the further reaction between the gas products (such as CO, H_2) and the O_2 is potentially occurs to produce the CO_2 and H_2O. The gasification process expecting lower CO_2, and based on the result it can be considered about the effect of O_2 excess in the gasification process. The more O_2 on the gasification process could potentially forming the more CO_2. In order to avoid these conditions, controlling the sufficient of O_2 supply for gasification process is important.

Those thus results above are initial information based on the model simulation development. These information are considerably to be applied to get better application on combustion and gasification processes. And finally, this

model is expected could be applied for further development of coal combustion and gasification.

NOMENCLATURE

Roman Symbol

h_s	Heat source (W/m^2 K)
A	Pre- exponential factor (unit vary)
A_p	Surface area of particle (m^2)
C_g	Reactant gas concentration (kmol/kg)
D_m	Diffusion coefficient (m^2/s)
E_a	Activation Energy (J/kmol)
F	External force (N)
M_i	Molecular weight of species i
M_w	Molecular weight of solid reactant
R	Gas universal constant (J/kmol K)
Y_i	Mass fraction of species i
k_i	Reaction rate coefficient for i
k_m	Mass transfer coefficient
m_i	Mass fraction
p_{ij}	Rate exponent of reacting species
h	Enthalpy (kJ/kg)
J_i	The flux of species i
S_m	Source of mass (kg)
S_h	Sherwood number
T	Temperature (K)
YY	Mass stoichiometric coefficient
M	Mass of particle (kg)
p	Pressure (Pa)
r	Rate consumption of reactant (kg/s)
$C_{\varepsilon 1}$; $C_{\varepsilon 2}$	Model constant
t	Time (s)
x	Distance/displacement (m)
u	Velocity (m/s)

Greek Symbol

α_i	Particle volume fraction
β	Temperature exponent
τ_{ij}	Stress tensor
$\emptyset$	Ratio of stoichiometric of solid and gas reactant
ρ	Density (kg/m^3)
ρg_i	Gravitational body force
μ	Viscosity (kg/m.s)
σ	Turbulent Prandtl number
δ	Kronecker delta

Subscript

p	Particle
i, j	Species or phase
vm	Volatile matter
k	Turbulent kinetic energy (m^2/s^2)
ε	Turbulent dissipation rate (m^2/s^3)

ACKNOWLEDGEMENTS

REFERENCES

[1] DOE/EIA, *International Energy Outlook 2016.* US Energy Information Administration, 2016. **0484**.

[2] Levendis, Y.A.J., Kulbhushan. Khatami, Reza. Sarofim, Adel F., *Combustion behavior in air of single particles from three different coal ranks and from sugarcane bagasse.* Combustion and Flame, 2011. **158**(3): p. 452-465.

[3] *Fluent 6.3 user's guide.* Fluent Inc., 2005.

[4] Chen X, h.M., Kojima T. , *Numerical simulation of entrained flow coal gasifiers.* Chem Eng Sci, 2000. **55 : 3861-74**.

[5] AM., M., *The rate of reduction of carbon dioxide by graphite.* Am Chem Soc J, 1934. **56:70–6.**

[6] Zogala, A., *CRITICAL ANALYSIS OF UNDERGROUND COAL GASIFICATION MODELS. PART II: KINETIC AND COMPUTATIONAL FLUID DYNAMICS MODELS.* Journal of Sustainable Mining, 2014.

[7] Alganash, B., M.C. Paul, and I.A. Watson, *Numerical investigation of the heterogeneous combustion processes of solid fuels.* Fuel, 2015. **141**: p. 236-249.

[8] Sun, Z., Wu, J., Wang, Y., Zhang, D. , *A kinetic study of CO2 gasification of a Chinese coal char during combined coal gasification and CH4 reforming.* Journal of Fuel Chemistry and Technology, 2009.

[9] Żogała, A. and T. Janoszek, *CFD simulations of influence of steam in gasification agent on parameters of UCG process.* Journal of Sustainable Mining, 2015. **14**(1): p. 2-11.

[10] Zikanov, O., *Essential Computational Fluid Dynamics.* 2012.

[11] Piyush Thakre, R.R., *Setting up Coal Combustion in STARCCM+5.04.* 2010.